

# Regulation of p53 activity through lysine methylation

Sergei Chuikov<sup>1</sup>, Julia K. Kurash<sup>2</sup>, Jonathan R. Wilson<sup>3</sup>, Bing Xiao<sup>3</sup>, Neil Justin<sup>3</sup>, Gleb S. Ivanov<sup>2</sup>, Kristine McKinney<sup>4</sup>, Paul Tempst<sup>5</sup>, Carol Prives<sup>4</sup>, Steven J. Gambelin<sup>3</sup>, Nikolai A. Barlev<sup>2</sup> & Danny Reinberg<sup>1</sup>

<sup>1</sup>Howard Hughes Medical Institute, Division of Nucleic Acids Enzymology, Department of Biochemistry, Robert Wood Johnson Medical School, Piscataway, New Jersey 08854, USA

<sup>2</sup>Molecular Oncology Research Institute, NEMC-Tufts School of Medicine, 75 Kneeland Street, Boston, Massachusetts 02111, USA

<sup>3</sup>Structural Biology Group, MRC-NIMR, The Ridgeway, Mill Hill, London NW7 1AA, UK

<sup>4</sup>Department of Biological Sciences, Columbia University, New York, New York 10027, USA

<sup>5</sup>Molecular Biology Program, Memorial Sloan Kettering Cancer Center, 1275 York Avenue, New York, New York 10021, USA

**p53 is a tumour suppressor that regulates the cellular response to genotoxic stresses. p53 is a short-lived protein and its activity is regulated mostly by stabilization via different post-translational modifications. Here we report a novel mechanism of p53 regulation through lysine methylation by Set9 methyltransferase. Set9 specifically methylates p53 at one residue within the carboxyl-terminus regulatory region. Methylated p53 is restricted to the nucleus and the modification positively affects its stability. Set9 regulates the expression of p53 target genes in a manner dependent on the p53-methylation site. The crystal structure of a ternary complex of Set9 with a p53 peptide and the cofactor product S-adenosyl-L-homocysteine (AdoHcy) provides the molecular basis for recognition of p53 by this lysine methyltransferase.**

Various histone modifications such as phosphorylation, acetylation, methylation and ubiquitination have been implicated in the regulation of gene expression by several mechanisms. The interplay between these modifications has been studied in detail and a 'histone code' hypothesis has been proposed to explain the effects of these modifications on gene expression<sup>1</sup>. Recently, we identified a histone methyltransferase, Set9, that targets histone H3 at lysine 4 and showed that this modification is associated with gene activation<sup>2,3</sup>. Here we demonstrate that Set9 activity is not limited to histones, it is also able to methylate the tumour suppressor p53.

p53 is a transcription factor that is mutated in approximately 50% of human cancers. In normal cells, p53 exerts a pivotal role in controlling the cell cycle, apoptosis and DNA repair in response to various forms of genotoxic stress. The regulation of p53 is complex and occurs mainly at the post-translational level<sup>4</sup>. This complexity is realized through the number and types of different post-translational modifications that contribute to its stabilization and activation. Phosphorylation of several residues at the amino terminus of p53 has been shown to affect its interaction with MDM2, which targets p53 for ubiquitin-mediated degradation<sup>5-7</sup>. The C terminus of p53 is rich in lysines, which are subjected to acetylation, ubiquitination and sumoylation<sup>4</sup>. Acetylation of the C terminus has been shown to protect p53 from ubiquitination<sup>8</sup>. Moreover, acetylation of p53 at lysines 373 and 382 increases its DNA-binding activity<sup>9,10</sup> and potentiates its interaction with other transcription factors<sup>11</sup>. The positive effects of acetylation on p53 activity can be reversed by deacetylation<sup>12</sup>. p53 has also been shown to be sumoylated at K386, although the exact role of this modification in the regulation of p53 is not yet clear<sup>13-15</sup>. Taken together, these data suggest very complex regulatory mechanisms, the coordination of which still remains elusive.

## p53 methylation by a lysine-specific methyltransferase Set9

Several enzymes that methylate specific lysine residues within the histone tails—histone lysine methyltransferases (HKMTs)—have been isolated and characterized. One such enzyme is Set9 (also known as Set7), which targets lysine 4 of histone H3 (H3-K4) *in vitro*<sup>2,3</sup>. However, purified Set9 was unable to methylate H3-K4 assembled into nucleosomes (Fig. 1a), which are thought to be the

physiologically relevant substrates for chromatin-modifying enzymes. However, methylation of nucleosomal H3-K4 does exist *in vivo*, but is catalysed by other enzymes, such as Set1 in yeast and by the related Set1, Ash1, SMYD3, trithorax and MLL proteins in higher eukaryotes. We therefore searched for additional candidate protein substrates, other than the histone polypeptides, that may be targeted by Set9 for methylation. We found that, in addition to several polypeptides (data not shown), Set9 methylated the tumour suppressor protein p53 *in vitro* (Fig. 1a). Under our assay conditions Set9-mediated methylation of p53 appeared to be quite specific. Other polypeptides such as cytochrome *c*, Gal4-VP16, bovine serum albumin (BSA) and  $\gamma$ -globulin did not serve as Set9 substrates (Fig. 1b). Moreover, other protein methyltransferases, such as Suv39H1, which targets H3-K9, PR-Set7 that targets H4-K20, or the arginine methyltransferase PRMT1, failed to use p53 as a substrate (Fig. 1c). Interestingly, recent studies have indicated that Set9 can methylate TAF10 (ref. 16), and although our studies did not address TAF10, the results collectively suggest that Set9-mediated methylation of proteins other than histone may be more general.

To gain insight into the role of p53 methylation, we first mapped the residue of p53 methylated by Set9. The initial analysis was performed using three fragments of p53 encompassing its functional domains: the N terminus (residues 1–82) representing the transactivation domain; the middle part of the protein containing the DNA-binding domain (residues 96–312); and the regulatory C terminus of the protein (residues 290–393). Set9 methylated p53 within the regulatory C terminus (data not shown). Next, the C terminus was further divided into three protein fragments (Fig. 1d, left panel) and each was analysed for methylation by Set9. The most C-terminal fragment, extending over amino acids 363 to 394, was a substrate for methylation (Fig. 1d, right panel, compare lanes 1–3). This polypeptide contained six lysines, which were then substituted individually, or in combination, with non-methylatable arginines and tested as substrates for methylation. We found that Set9 methylated lysine 372 (lanes 4–7). Consistent with this observation, a single substitution at lysine 372 with arginine in the full-length p53 protein eliminated methylation by Set9 (Fig. 1e). These data established that the site of Set9 methylation is within a region of the

p53 protein that is subjected to multiple post-translational modifications (Fig. 1f). This arrangement of amino acids, subjected to different post-translation modifications, resembles the arrangement within the histone tails, wherein one modification can affect another, an observation that has contributed in part to the proposal of a histone code hypothesis.

**Affinity of Set9 for p53 and H3-derived peptides *in vitro***

There is no obvious similarity between the p53 sequence surrounding its methylation site and sequences containing the sites methylated on H3 at K9, K27, K36 or H4 at K20 (Fig. 2a). On the other hand, comparison between the H3-K4 and p53 sequences shows some degree of amino-acid conservation around the methylation site. Moreover, if the amino-acid sequence present in TAF10, a substrate of Set9 (ref. 16), is included in the analysis, the Set9 local recognition sequence appears to be restricted to three residues R/K-S/T-K (Fig. 2a). The affinity of Set9 for putative peptide substrates derived from the sequences of either the H3 tail or p53 was determined by competition binding studies against an N-terminal dansyl-labelled H3 10-mer peptide (Fig. 2b). Notably, the affinity of

the p53 20-mer was 12-fold higher than the equivalent H3 20-mer (a dissociation constant ( $K_d$ ) of 0.2  $\mu$ M compared to 2.4  $\mu$ M, respectively). The tighter affinity for the p53 20-mer substrate correlated with a sixfold increase in enzymatic activity, as measured by methyltransferase assays with  $^3$ H-labelled S-adenosyl-L-methionine (AdoMet) (data not shown). As with the H3 peptide<sup>17</sup>, Set9 mono-methylated the target lysine residue of p53 (Supplementary Fig. S1).

**The ternary structure of Set9 with a peptide derived from p53**

We next determined the structure of Set9 in complex with a mono-methylated p53 peptide and the cofactor product AdoHcy. We compared this structure to the previously solved complex of Set9 with mono-methylated H3 peptide<sup>17</sup>. Well-ordered crystals of the p53 peptide ternary complex were obtained that diffracted to better than 1.8-Å resolution. The structure was solved by molecular replacement and relevant crystallographic statistics are given in Supplementary Table T1.

The overall structure of the complex, shown in ribbon representation in Fig. 2c, is similar to that obtained for the Set9-H3 ternary complex (Protein Data Bank (PDB) code 1o9s). An overlay of Set9

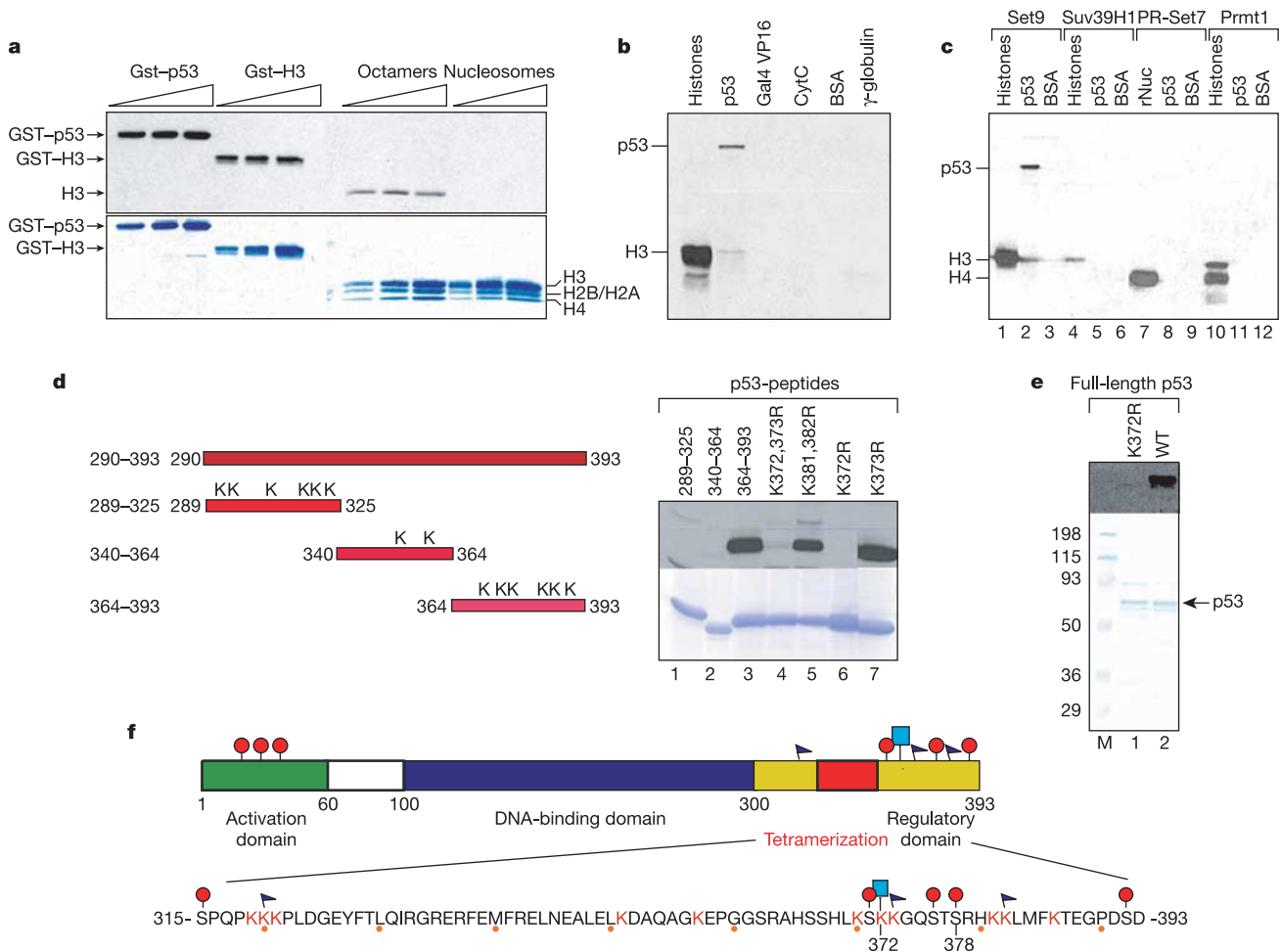


**Figure 1** Set9 methylates p53 *in vitro*. **a**, Increasing amounts of GST-p53, GST-H3, histone octamers and recombinant histone nucleosomes were methylated by Set9, separated by 12% SDS-polyacrylamide gel electrophoresis (PAGE) transferred onto PVDF membrane, sprayed with EN<sup>3</sup>HANCE and exposed to film (top). Coomassie-blue staining of the gel shown above (bottom). **b**, 3  $\mu$ g of core histones, p53, Gal4-Vp16, cytochrome c, BSA or  $\gamma$ -globulin were tested as substrates for methylation by Set9, separated by 12% SDS-PAGE, and analysed by autoradiography. **c**, 3  $\mu$ g of recombinant histone octamers (recombinant nucleosomes for PR-Set7), full-length p53 and BSA were tested as

substrates for methylation by Set9, Suv39H1, PR-Set7 or PRMT1 as indicated. **d**, Schematic representation of the C-terminal p53 peptides and lysine candidates for methylation (left). Methylation assay with the wild-type and mutant p53 peptides (right). **e**, Autoradiogram of methylation assay with full-length p53 WT and K372R mutant (top). Coomassie-blue staining of the methylation assay gel shown above (bottom). **f**, Schematic representation of the p53 domain structure and post-translational modifications at the C terminus. Circles, flags and the rectangle represent phosphorylation, acetylation and methylation of p53, respectively.

ternary structures with p53 or H3 substrates shows a strong overall similarity between the two (ribbons representation in Supplementary Fig. S2). Importantly, the mono-methylated lysine side-chain of the p53 peptide accesses the methyl donor cofactor using the same narrow channel running through the SET domain as that described for the H3 complex. Overall, the electron-density map for the Set9–p53 complex is of high quality. There is well-resolved electron density for the first six residues of the p53 peptide, for residues Leu (–3) to Gly (+2) (numbering is with respect to the modified p53 lysine residue 372) but the last four residues of the peptide are disordered. This observation suggests that Set9 interacts with a rather short recognition sequence at the active site of the enzyme. The Set9 residues involved in interactions with the three amino acids that are N-terminal to the modified lysine are the same for the p53 peptide and the H3 peptide despite the difference in peptide sequence (Fig. 3d). The hydrogen bond between the carbonyl of Arg 258 and the Ne atom of Arg (–2) in the H3 complex is replaced by a hydrogen bond with the Ne of Lys (–2) in p53. The hydrophobic packing of Trp 260 with the peptide Arg (–2) in H3 is substituted with the packing against Lys (–2) in p53. There is also a conservative substitution of Ser (–1) in H3 for Thr (–1) in p53 that maintains the hydrogen bond with Ser 268 of the enzyme.

Of the five Set9 residues making polar contacts with the peptide, four of them—Asp 256, Arg 258, Thr 266 and Ser 268—are located

within the variable Set-I region. The sixth residue making a polar contact with the peptide is located in the C-flanking domain (Tyr 335). Together, these observations highlight the significance of the variable Set-I and C-flanking domains in determining the specificity of the SET enzymes with respect to which lysine residue within a stretch of polybasic residues will be modified. The binding studies reported before also indicated that there must be amino-acid residues located at some distance from the target lysine residue that play an important role in determining substrate specificity. Although no structural data are available for the interactions formed between these more distant residues with Set9, it is tempting to speculate that the N-flanking domain, preceding the SET domain, may be involved in mediating these interactions.

### p53 is methylated *in vivo*

To facilitate studies on the role of Set9-methylation of p53 *in vivo*, we generated a polyclonal antibody that specifically recognized mono-methylated p53-K372. Rabbit antibodies were initially screened against p53 peptides harbouring K372 with different degrees of methylation. An antibody that specifically recognized a mono-methylated peptide, but failed to detect an unmodified peptide or equivalent peptides that were di- or tri-methylated was selected (Fig. 3a). The anti-p53-K372-mono-methyl (anti-p53-K372me) antibody specifically detected bacterially purified p53

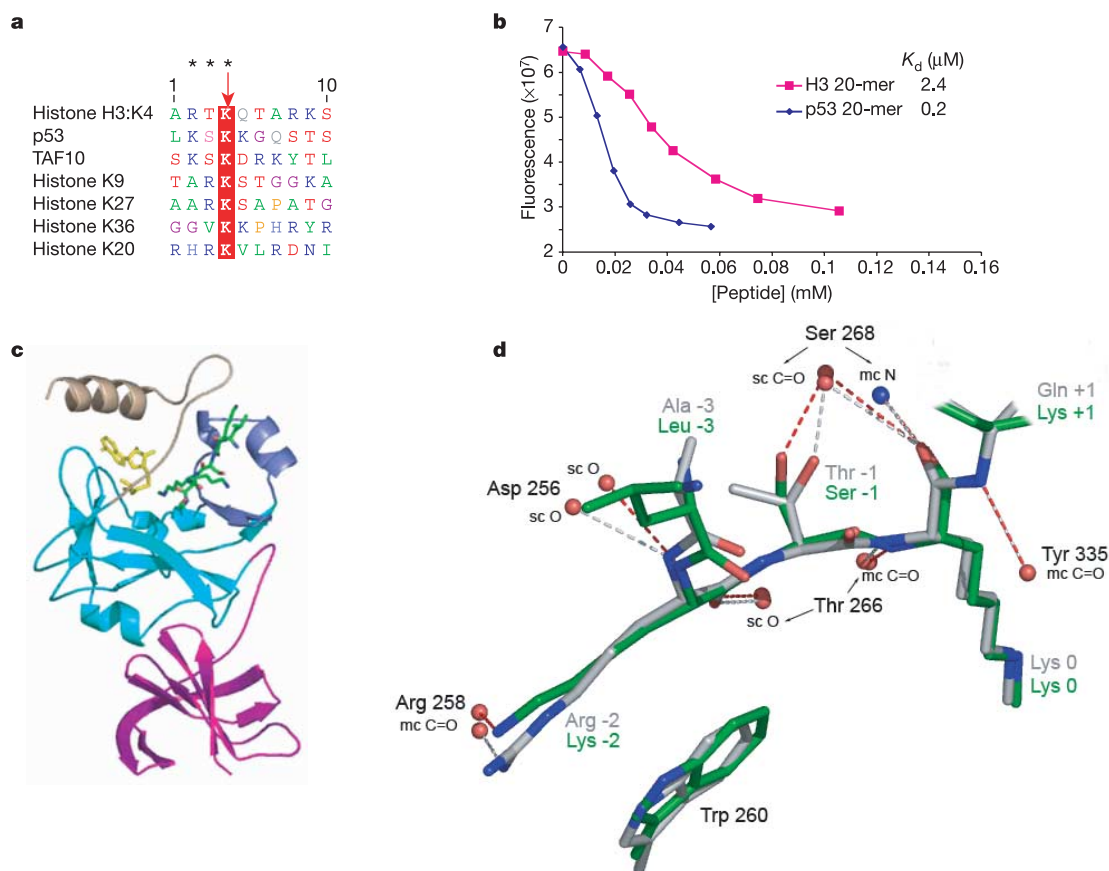


**Figure 2** Interaction of Set9 with p53 and H3 peptides. **a**, Alignment of protein sequences adjacent to lysines targeted for methylation in the case of histone H3 lysine 4, p53, TAF10, histone H3 lysine 9, histone H3 lysine 27, histone H3 lysine 36, and histone H4 lysine 20. Methylated lysine is highlighted in red and the asterisk represents the consensus for substrate recognition by Set9 methyltransferase. **b**, The dissociation constants of the p53 and H3 peptides, shown in inset, were determined using fluorometric competition assay. The unlabelled p53 and H3 peptides were used to displace a dansyl-labelled H3 10-mer of known affinity. The displacement curves were used to calculate the dissociation

constants of the unlabelled peptides (shown in inset). **c**, Overall structure of the Set9–p53 complex. Magenta, N-flanking domain; cyan, Set domain; blue, Set-I domain; beige, C-flanking domain. The backbone of the p53 peptide is green, and AdoHcy is yellow. **d**, Overlay of the peptide showing enzyme interactions for the Set9–p53 complex and the Set9/H3 complex. The p53 carbon atoms are shown in green and H3 in grey. Hydrogen bonds are represented by dashed lines: only the Set9 donor/acceptor atoms are shown for each complex.

protein methylated by Set9 *in vitro*, but was severely compromised with the untreated p53 protein. Equivalent amounts of methylated and mock-methylated p53 were used in the western analysis (Fig. 3b). We concluded that the antibody specifically recognized K372-methylated p53.

To address the question of whether p53 is methylated by Set9 *in vivo*, wild-type Set9 or its catalytically inactive mutant form (H297A) were stably transfected into 293F cells expressing endogenous p53. Western-blot analysis using anti-p53-K372me antibody detected methylated p53 protein in extracts derived from cells overexpressing the wild-type Set9 protein, but cells overexpressing the catalytically inactive Set9 protein displayed little methylated p53 (Fig. 3c). The expression levels of Set9 proteins and the amounts of p53 protein in the extracts were similar (Fig. 3c, bottom panels). We therefore concluded that transfected Set9 methylated p53 in 293F cells.

We next examined p53 methylation at lysine 372 *in vivo* under conditions in which the intracellular concentration of Set9 was unaltered. 293F cells were treated with adriamycin (Adr), a chemical that induces DNA damage resulting in the activation of a p53-responsive pathway. Cell extracts prepared from untreated and Adr-treated cells, were then compared for total amounts of p53 protein using monoclonal p53 antibody. Under these conditions, DNA damage did not increase the levels of intracellular p53; this is not surprising because p53 is already stabilized by adenoviral proteins expressed endogenously in 293F cells<sup>18</sup>. Both extracts were also subjected to immunoprecipitation with anti-p53-K372me antibodies followed by western blotting with p53-specific antibody. Adr treatment increased the intracellular concentration of methylated K372-p53 protein (Fig. 3d). Importantly, the levels of Set9 remained unchanged after Adr treatment (data not shown). p53 also became methylated in response to DNA damage in U2OS cells (Fig. 3e). Importantly, the introduction of Set9 short interfering (si) RNA in these cells decreased K372 methylation of p53 upon

Adr treatment (Fig. 3e) and correlated with the decreased levels of Set9 (see Fig. 4c). These findings collectively suggested that methylation of p53 in response to DNA damage is a general phenomenon, rather than a cell-type-specific event.

**Methylated p53 is in the nucleus and regulates p53 target genes**

In our initial attempt to characterize the function of p53-K372 methylation, we stably transfected 293F cells with a Set9 expression vector. Extracts from these cells were then fractionated into nuclear and cytosolic fractions to determine the distribution of methylated p53-K372. These studies suggested that all the methylated p53-K372 was localized to the nucleus, although p53 was equally distributed between the nuclear and cytosolic fractions (Fig. 4a). Importantly, untransfected 293F cells also displayed methylated p53 in the nuclear fraction, ruling out the possibility that the nuclear localization of methylated p53-K372 is a consequence of Set9 overexpression.

We next analysed whether Set9-mediated methylation of p53 affected its transcriptional activity. We focused on one of the best-characterized p53 transcriptional targets, the *p21/WAF/CIP* gene, whose product is critical for cell-cycle arrest in the G1 phase. The effect of Set9-mediated p53-K372 methylation on transcription of the endogenous p21 gene was measured in U2OS cells using reverse-transcription polymerase chain reaction (RT-PCR). Overexpression of Set9 (Fig. 4b, middle panel), resulted in increased expression of p21 (Fig. 4b, left panel), and correlated with increased levels of K372-methylated p53 (Fig. 4b, right panel). Importantly, even in the absence of DNA damage, the levels of p21 expression in cells overproducing Set9 were higher than those in the parental non-transfected cells treated with the DNA-damaging agent (Fig. 4b, compare lane 4 with lane 1). As expected, overexpression of Set9 followed by Adr treatment resulted in a further increase in the levels of p21 expression (Fig. 4b, lane 3).

We directly analysed the contribution of Set9 to regulation of p21

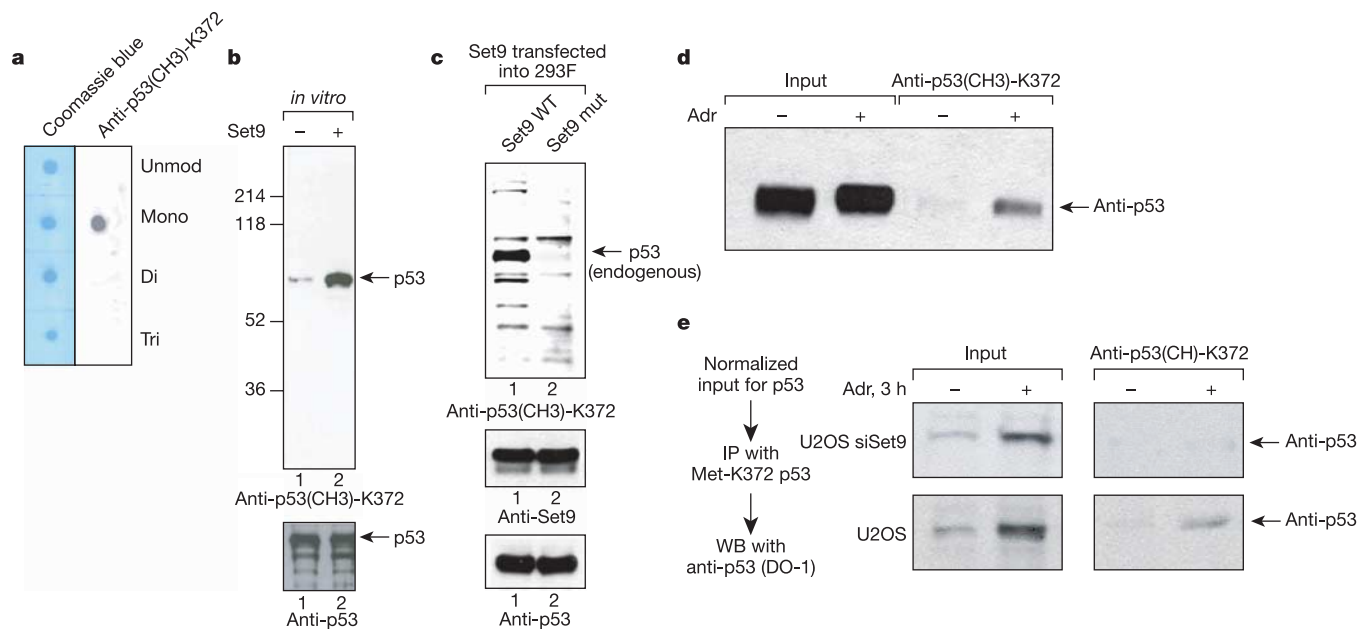


**Figure 3** Set9 methylates p53 *in vivo*. **a**, Dot blot assay of the p53 peptides containing various degrees of methylation. Equal amounts of unmodified, mono-, di- and tri-methylated p53 peptides were immunoblotted with mono-methyl p53 antibody (right panel). Coomassie-blue staining of these peptides served as a loading control (left). **b**, Western-blot analysis of recombinant p53 methylated by Set9 *in vitro* using mono-methyl p53 antibody (top). Western-blot signal using anti-p53 antibody served as a loading control (bottom). **c**, Detection of endogenous methylated p53 from whole-cell extracts of 293F stable cell lines overexpressing wild-type (WT) or mutant (mut) Set9.

Methylated p53 was detected by western blotting with anti-p53K372me antibody (top). Western-blot signals obtained with anti-Set9 and anti-p53 antibodies served as loading controls. **d**, Immunoprecipitation of methylated endogenous p53 from nuclear extracts of 293F cells treated or mock-treated with Adr with anti-p53K372me Ab. Western blot with anti-p53 antibody (DO-1) is also shown. **e**, U2OS cells with or without Set9 siRNA were treated with 0.5 μM of Adr for 3 h. Nuclear extracts from treated or mock-treated cells were normalized for the amounts of total p53 and subjected to immunoprecipitation (IP) with anti-p53K372me antibody. Western blot with anti-p53 antibody (DO-1) is shown.

expression. The levels of p21 expression in U2OS cells stably expressing ectopic Set9 were approximately twofold higher than in the parental strain. Consistent with the results presented in Fig. 4b, a similar pattern of p21 expression was observed upon treatment of cells with 5FU (a compound that also induces DNA damage), that is, in the presence of Set9 overexpression the levels of p21 increased over twofold compared to the parental cells. Strikingly, overexpression of a catalytically inactive form of Set9 completely ablated the induction of p21 in response to DNA damage (Fig. 4c). Most importantly, si-RNA-mediated reduction of the intracellular levels of Set9 also impaired p21 expression upon DNA damage in U2OS cells (Fig. 4c). These findings collectively established that Set9 is required, directly or indirectly, for the expression of p21. Surprisingly, the introduction of either the Set9 mutant or si-RNA against Set9 protein also decreased the total levels of p53, without affecting

the expression of unrelated proteins, such as tubulin (Figs 4c and 5b). The observed stimulatory effect of Set9 on p21 gene expression extended to other p53-responsive genes such as BAX and MDM2 (Supplementary Fig. S3).

### Increased stability of methylated p53-K372

That the intracellular levels of p53 were critically dependent on the enzymatic activity of Set9 suggested that methylation of p53-K372 might affect p53 stability. We directly tested this hypothesis with pulse-chase experiments. U2OS cells were transiently transfected with wild-type or a catalytically inactive Set9 and grown in a methionine-free medium in the presence of <sup>35</sup>S-methionine for 30 min. The cells were then washed, resuspended in media containing methionine and then a fraction of the cells were withdrawn at the indicated times. The amount of <sup>35</sup>S-radiolabelled p53 in the

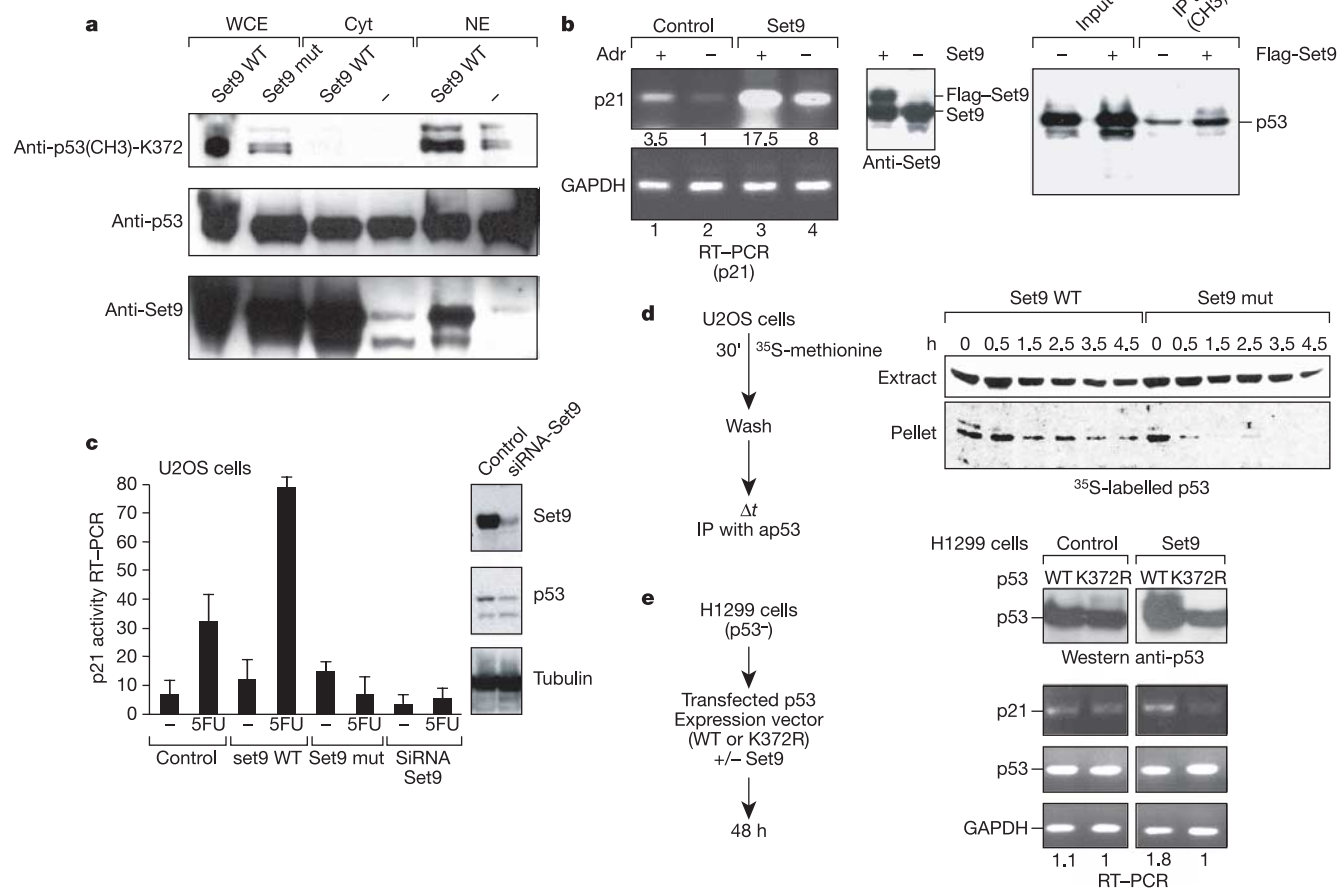


**Figure 4** Set9 potentiates p53 function. **a**, 293F cells stably expressing Set9 were lysed and whole-cell extract, cytoplasmic and nuclear fractions were prepared. Top, western-blot analysis of methylated p53 with anti-p53K372me antibody; middle, western-blot analysis of total p53 with anti-p53 antibody (served as a loading control); bottom, western-blot analysis of Set9. **b**, RT-PCR of p21 gene expression in U2OS cells with normal or overexpressed amounts of Set9 after treatment with the DNA-damaging agent Adr (left). Shown are the relative values normalized to the p21 signal in untreated U2OS cell. U2OS cells were stably transfected with Flag-Set9 wild type, or mock-transfected. Western-blot analysis of the endogenous and ectopic Set9 proteins expressed in U2OS cells. Non-transfected cells were used as control (middle panel). Endogenous p53 was immunoprecipitated with anti-p53K372me antibody from nuclear extracts of U2OS cells transiently transfected with either Flag-Set9 or control constructs. Western-blot analysis of p53 levels in both types of cells with anti-p53 antibody (DO-1) is shown. Input lanes represent 10% of the starting amounts of p53 in both cell lines. IP lanes show the amounts of methylated p53 immunoprecipitated from these cell lines (right panel). **c**, U2OS cells

were stably transfected with Flag-Set9 WT, Flag-Set9 mutant and siRNA against Set9. Non-transfected cells served as control. Cells were mock-treated, or treated with 0.3 μM of 5-fluoro-uracil (5-FU). p21 gene expression was analysed by quantitative real-time PCR using primers specific for the coding region. Shown are the relative values normalized to the GAPDH signal (left). Western-blot analysis of Set9 and p53 in U2OS cells before and after transfection with siRNA against Set9 (right, upper and middle, respectively). Tubulin was used as a loading control (right, bottom). **d**, U2OS cells transiently transfected with Set9 WT or Set9 mutant and labelled with <sup>35</sup>S methionine. At the indicated times, cells were lysed and both soluble and insoluble fractions were immunoprecipitated separately with anti-p53 antibody. The immunoprecipitates were resolved by SDS-PAGE and visualized by autoradiography. **e**, Wild-type or K372R mutant of p53 were co-transfected with Set9 WT or control vector into H1299 cells. After 48 h, cells were collected and analysed for p53 protein levels by western blotting (top) and for p53 and p21 gene expression levels by RT-PCR (bottom). The level of GAPDH expression served as control. Shown are the relative values normalized to the levels of p21 activated by p53 K372R.

cytosolic and nuclear pellet fractions was analysed by immunoprecipitation of p53 using monoclonal antibody. The stability of nuclear p53 increased in cells expressing wild-type Set9, but not in cells expressing a catalytically inactive form of Set9 (Fig. 4d). Consistent with our findings that methylated p53-K372 is nuclear (Fig. 3a), p53 stabilization was apparent only in the fraction of nuclear p53 associated with chromatin (Fig. 4d). Thus, we concluded that Set9-mediated methylation of p53-K372 resulted in the stabilization of a chromatin-bound fraction of p53. This conclusion was supported by experiments performed in H1299 cells lacking endogenous p53. Increased stabilization of wild-type p53, but not its methylation-defective mutant (K372R) was observed in these cells upon overexpression of Set9 (Fig. 4e, compare left and right panels). The expression levels of ectopic wild-type and K372R mutant p53 genes were similar, as shown by RT-PCR (Fig. 4e bottom), and thus cannot account for the observed difference in the

p53 protein levels. Moreover, Set9 overexpression resulted in increased expression of the *p21* gene specifically in the presence of wild-type p53, but not with the K372R mutant (Fig. 4e bottom), confirming that Set9 regulates p53-dependent genes through p53 methylation at K372.

We speculated that, given that overexpression of wild-type Set9 resulted in ‘hyper-stabilization’ and activation of nuclear p53, induction of cell-cycle arrest and apoptosis should ensue. We directly tested this hypothesis by measuring the p53-dependent apoptotic response induced by DNA damage. Consistent with previous reports, treatment of U2OS cells with Adr increased the number of cells positively stained for Annexin V (Fig. 5a, compare panels 1 and 2). Importantly, cells overexpressing Set9 exhibited higher apoptotic staining even without DNA damage (compare panels 3 and 1). The treatment of Set9-overexpressing cells with Adr further increased the Annexin V staining (compare panels 3 and 4). Overexpression of the catalytically inactive Set9 abrogated DNA-damage-induced apoptosis, suggesting that the methyltransferase activity of Set9 is critical for induction of p53-dependent apoptosis (Fig. 5a, compare panels 5 and 6). Again, the overexpression of a catalytically inactive Set9 mutant protein resulted in decreased p53 levels, confirming a functional interaction between p53 and Set9 (Fig. 5b). Importantly, Set9-mediated regulation of cell cycle and apoptosis was p53-dependent, because in the absence of p53 transfected Set9 was unable to induce p21 gene expression in H1299 (Supplementary Fig. S4) or apoptosis in Saos-2 cells in response to DNA damage (Supplementary Fig. S5).

Next, we tested whether p53 methylated by Set9 is present at the promoters of p53 target genes. Our work suggested that p53 methylation is likely to precede acetylation (manuscript in preparation). Therefore, we reasoned that p53 methylation must occur at very early times after DNA damage. To test this hypothesis, we treated normal U2OS and Set9-siRNA-expressing cells with Adr at different times (Fig. 6). At the indicated time periods, cells were harvested, and DNA-protein complexes were cross-linked and subjected to chromatin immunoprecipitation (ChIP) analysis, initially using anti-p53-K372me antibodies. To increase the specificity of ChIP, the anti-p53-K372me immunoprecipitates were eluted from the beads with 1% SDS, diluted with immunoprecipitation buffer and then subjected to a second round of immunoprecipitation using anti-p53 antibody. Consistent with our hypothesis, the amount of methylated p53 bound to the p21 promoter increased as early as 1.5 h after DNA damage. Importantly, K372 methylation was Set9-specific, because U2OS cells expressing siRNA against Set9 did not exhibit a significant increase in methylated p53 at the p21 promoter. These results suggested that methylation of p53, in addition to acetylation and phosphorylation, may represent an important DNA-damage-induced modification mark required for p53 function *in vivo*.

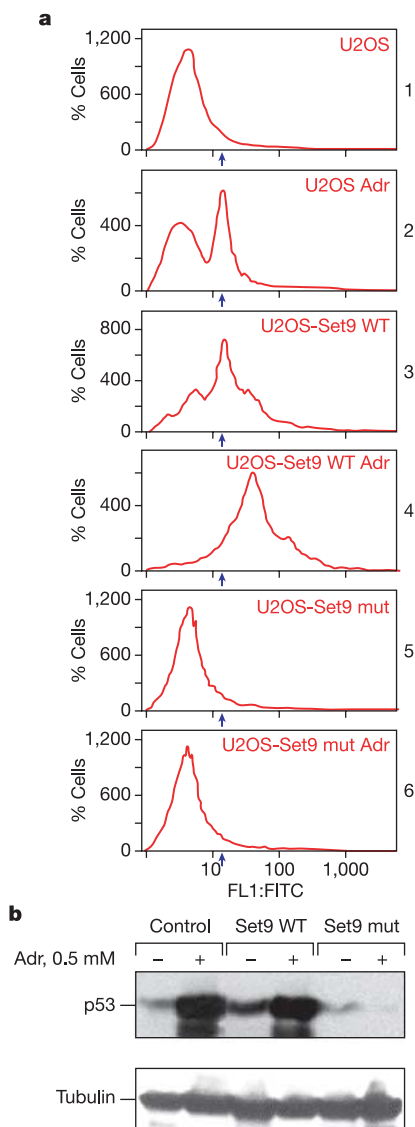


**Figure 5** Set9 increases apoptosis in U2OS cells. **a**, The efficiency of apoptosis was determined by Annexin V-fluorescein isothiocyanate (FITC) staining. U2OS stably expressing Set9 WT or Set9 mutant were treated with 0.5  $\mu$ M Adr for 24 h or untreated. Non-transfected cells were used as control. Cells were stained with propidium to eliminate necrotic cells and with Annexin V-FITC to score for apoptotic cells. Arrows show the peak of apoptotic cells. **b**, Western-blot analysis of p53 in whole-cell extracts from U2OS cells stably expressing Set9 WT or its catalytically inactive mutant (top). Western-blot signal of tubulin was used as a loading control (bottom).

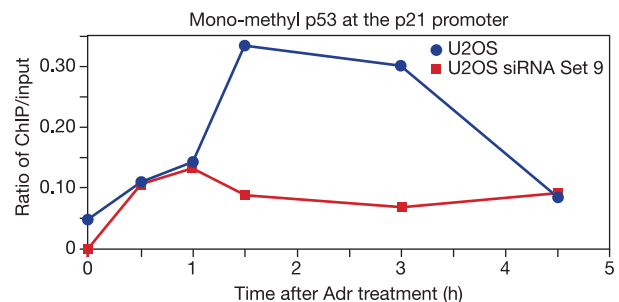


**Figure 6** Methylation of p53 at the p21 promoter. U2OS and U2OS Set9 siRNA cells were treated with 0.5  $\mu$ M of Adr and collected at the indicated time points for ChIP assay performed using anti-p53K372me antibody. The amounts of precipitated p21 promoter were determined by quantitative RT-PCR as described above.

Here we have established that Set9 methylates p53 at a specific lysine residue *in vivo*. Importantly, we found that this methylation is required for p53 stabilization. What is the mechanism for methylation-induced stabilization of p53? One of the possibilities is that methylation interferes with MDM2-mediated ubiquitination of the six lysine residues at the C terminus, which leads to subsequent p53 degradation and/or nuclear export<sup>4</sup>. Yet, because of its small size, the mono-methylation mark itself is unlikely to affect ubiquitination. We speculate that similar to histones, as-yet-unidentified factors may bind methylated p53 and interfere with Mdm2-dependent ubiquitination. Overexpression of the catalytically inactive Set9 mutant decreased intracellular levels of p53 and attenuated its activity. This confirms the functional connection between Set9 and p53 and also highlights another possible mechanism for p53 inactivation in human cancers. Finally, based on the observation that p53 is a better substrate for Set9 than histone H3, we propose that Set9 might regulate the function of other factors. Likewise, the activities of other known lysine methyltransferases may not be limited to histones, but may also target factors important in many cellular processes. In this regard, the ternary complex of Set9 with p53 reveals the molecular basis for Set9 substrate recognition and may lead to the identification of new Set9 targets in the future. □

## Methods

### Constructs

GST-H3 N-terminal peptide was expressed as described<sup>19</sup>. For GST-C-terminal p53, construct C-terminal (amino acids 290–393) was cloned into PGEX3 vector (Promega). For methylation site identification, different p53 peptides (aa 290–235, 340–364, 364–393) were cloned into Pet102 (Invitrogen) vector and expressed in *Escherichia coli* as a thioredoxin fusion proteins.

### Peptides

The following peptides were chemically synthesized for antibody production and dot blots.

p53 unmodified: NH<sub>2</sub>-CSHLKSKKGQST-COOH; p53 mono-methyl-K372: NH<sub>2</sub>-CSHLKSK-(Me)KGQST-COOH; p53 di-methyl-K372: NH<sub>2</sub>-CSHLKSK-(Me<sub>2</sub>)KGQST-COOH; p53 tri-methyl-K372: NH<sub>2</sub>-CSHLKSK-(Me<sub>3</sub>)KGQST-COOH.

### Methylation assay

Methylation assay was performed as described previously<sup>3</sup>.

### Stability assays

U2OS cells were transfected with Set9 WT or mutant 36 h before labelling. 24 h after transfection, cells were split into 60-mm plates to 50% confluence. Next morning, cells were washed twice with PBS and preincubated for 30 min with DMEM (without methionine) containing 5% dialysed FCS. Cells were labelled for 30 min in fresh methionine-free DMEM containing 0.5 mCi of <sup>35</sup>S methionine. Radioactive media were then removed and cells were washed with PBS, followed by the addition of DMEM containing FCS, and 2 mM methionine. At the indicated times cells were washed with PBS and collected. Cytoplasmic and nuclear fractions were prepared as described<sup>3</sup> and p53 was immunoprecipitated from each fraction with p53-specific antibody (DO-1).

### siRNA construct and Set9 knock-down

For lentiviral vector-based knock-down, the desired 23 base pair (bp) stem-loop RNAs were expressed from the pLSL-GFP vector (a gift from P. Chumakov) driven by the human H1 gene promoter. The vector also contained a minimal histone H4 promoter that drives transcription of a green fluorescent protein (GFP) gene used to monitor infection efficiency. pLSL-GFP vectors expressing the following hairpin RNAs were co-transfected with packaging plasmids pCMV-VSVG and pCMV-deltaR8.2 into 293T cells on a 6-cm dish by standard calcium-phosphate precipitation. Viral supernatants were collected from the transfected 293T cells 24, 36 and 48 h post-transfection, filtered and used for infection of ~5 × 10<sup>4</sup> target U2OS cells grown on six-well plates in the presence of 4 μg ml<sup>-1</sup> of polybrene (Sigma). The U2OS cells were infected with >100% efficiency as judged by GFP fluorescence, expanded and used as a mass culture for all subsequent experiments.

The stem-loop siRNAs were synthesized as two complementary 67-nt oligos, annealed and cloned into *Bam*HI/*Eco*RI sites of pLSL-GFP vector. The siRNA oligo used to target SET9 is:

5' gatccgacctggagcatgacggattacctctctcaGTAATCCGTCATCGTCCAGGTCGctttttg-3' (targeted sequences are in upper case, the loop sequence between sense and antisense 23-mers is in lower case, restriction sites that overhang nucleotides are underlined).

### RT-PCR

Total RNA was extracted using the TRI reagent (Invitrogen) according to the manufacturer's instructions. First-strand complementary DNA was synthesized using Ready-To-Go You-Prime First-Strand Beads (Amersham Biosciences).

### Real-time PCR

Real-time PCR was performed with the DNA Engine Opticon 2 System (MJ Research) according to the manufacturer's instructions. The primers for human p21 (Cip1/WAF1<sup>1</sup>) and GAPDH (GenBank accession numbers NM\_000389 and NP\_002037 respectively) were designed using the Primer3 program. Primers for the p21 gene: 5'-CACCGAG ACACCACTGGAGG-3' and 5'-GAGAAGATCAGCCCGCTTT-3', GAPDH: 5'-GGGAAGGTGAAGTCCGGAGT-3' and 5'-TTGAGTCAATGAAGGGGTCA-3' were synthesized and purified by IDT DNA Technologies. Primer pairs were designed to amplify the appropriate DNA fragments using the following conditions: 10 min initial denaturation, followed by cycles of 1 min at 94 °C, 1 min at 62 °C and 1 min at 72 °C. Fluorescence was measured after the end of the elongation phase at 79 °C. Expression levels were calculated as a ratio between p21 and GAPDH signals. Correct PCR products were confirmed by agarose gel electrophoresis (2% w/v) and melting curve analysis.

### ChIP assay

ChIP assay on U2OS and U2OS cells expressing siRNA-Set9 was performed as described previously<sup>11</sup>. Briefly, cells were cross-linked with 1% formaldehyde, neutralized with 0.125 M glycine and harvested by scraping. The chromatin fraction was prepared by incubating the cells in lysis buffer (10 mM Tris pH 8.0, 200 mM NaCl, 10 mM EDTA, 0.5 mM EGTA, 1 mM PMSF). The insoluble fraction was sonicated and subjected to immunoprecipitation with anti-p53-K372me serum. Following washes, the immunoprecipitated material was eluted with 1% SDS and 10 mM DTT, diluted ten times and re-immunoprecipitated with anti-p53 serum. DNA was then isolated and subjected to real-time PCR as described above.

### Determination of the Set9 ternary complex with p53

The Set9 protein was prepared from a GST fusion as described previously<sup>17</sup>. A highly concentrated stock solution (100 mg ml<sup>-1</sup>) of Set9 (aa108–366) was prepared in 50 mM Tris-HCl, pH 7.0, 100 mM NaCl, and diluted to 10 mg ml<sup>-1</sup> with a twofold molar excess of p53 10-mer peptide mono-methylated at Lys4 and AdoHcy. Crystals were grown at 18 °C by vapour diffusion as hanging drops prepared by mixing equal volumes of protein complex with a reservoir solution containing 0.1 M Tris-HCl, pH 7.8 and 22% PEG 3350. Crystals were first transferred into mother liquor augmented with an additional 5% PEG 400, before plunging into liquid nitrogen. Data were collected from flash-cooled crystals at 100 K on an ADSC Q4R CCD detector at SRS Daresbury. Diffraction data were integrated and scaled using DENZO and SCALEPACK<sup>20</sup>. The structure was solved by molecular replacement using our previous model (1o9s.brk) with AMORE. Subsequent refinement was performed using REFMAC version 5.0 (ref. 21) and manual model building in O (ref. 22).

### Determination of p53 peptide affinities

The dissociation constants were determined using fluorometric competition assays. The p53 and H3 peptides were unlabelled and used to displace a dansyl-labelled H3 10-mer (ARTKQTARKY) of known affinity. The resulting displacement curves were used to calculate the K<sub>d</sub> of the unlabelled peptides: H3 20-mer (ARTKQTARKSTGGKAPRKQY) and p53 WT 20-mer (LKSCKGQSTSRHKKLMFKTY). These peptides were tested against the Set9 construct consisting of residues 52–366. Fluorescence measurements were made using a Spex Fluoromax spectrophotometer with 330 nm (excitation) and 520 nm (emission) wavelengths respectively. The titrations were performed at 20 °C in a buffer containing 25 mM Tris-HCl pH 8.0.

Received 17 August; accepted 13 October 2004; doi:10.1038/nature03117.

Published online 3 November 2004.

- Jenuwein, T. & Allis, C. D. Translating the histone code. *Science* **293**, 1074–1080 (2001).
- Wang, H. *et al.* Purification and functional characterization of a histone H3-lysine 4-specific methyltransferase. *Mol. Cell* **8**, 1207–1217 (2001).
- Nishioka, K. *et al.* Set9, a novel histone H3 methyltransferase that facilitates transcription by precluding histone tail modifications required for heterochromatin formation. *Genes Dev.* **16**, 479–489 (2002).
- Appella, E. & Anderson, C. W. Post-translational modifications and activation of p53 by genotoxic stresses. *Eur. J. Biochem.* **268**, 2764–2772 (2001).
- Shieh, S. Y., Ikeda, M., Taya, Y. & Prives, C. DNA damage-induced phosphorylation of p53 alleviates inhibition by MDM2. *Cell* **91**, 325–334 (1997).
- Momand, J., Wu, H. H. & Dasgupta, G. MDM2—master regulator of the p53 tumor suppressor protein. *Gene* **242**, 15–29 (2000).
- Brooks, C. L. & Gu, W. Ubiquitination, phosphorylation and acetylation: the molecular basis for p53 regulation. *Curr. Opin. Cell Biol.* **15**, 164–171 (2003).
- Li, M., Luo, J., Brooks, C. L. & Gu, W. Acetylation of p53 inhibits its ubiquitination by Mdm2. *J. Biol. Chem.* **277**, 50607–50611 (2002).
- Luo, J. *et al.* Acetylation of p53 augments its site-specific DNA binding both *in vitro* and *in vivo*. *Proc. Natl Acad. Sci. USA* **101**, 2259–2264 (2004).
- Gu, W. & Roeder, R. G. Activation of p53 sequence-specific DNA binding by acetylation of the p53 C-terminal domain. *Cell* **90**, 595–606 (1997).
- Barlev, N. A. *et al.* Acetylation of p53 activates transcription through recruitment of coactivators/histone acetyltransferases. *Mol. Cell* **8**, 1243–1254 (2001).
- Gu, W., Luo, J., Brooks, C. L., Nikolaev, A. Y. & Li, M. Dynamics of the p53 acetylation pathway. *Nov. Found. Symp.* **259**, 197–205 (2004).
- Gostissa, M. *et al.* Activation of p53 by conjugation to the ubiquitin-like protein SUMO-1. *Embo J.* **18**, 6462–6471 (1999).
- Kwek, S. S., Derry, J., Tyner, A. L., Shen, Z. & Gudkov, A. V. Functional analysis and intracellular localization of p53 modified by SUMO-1. *Oncogene* **20**, 2587–2599 (2001).
- Rodriguez, M. S. *et al.* SUMO-1 modification activates the transcriptional response of p53. *Embo J.* **18**, 6455–6461 (1999).

16. Kouskouti, A., Scheer, E., Staub, A., Tora, L. & Talianidis, I. Gene-specific modulation of TAF10 function by SET9-mediated methylation. *Mol. Cell* **14**, 175–182 (2004).
17. Xiao, B. *et al.* Structure and catalytic mechanism of the human histone methyltransferase SET7/9. *Nature* **421**, 652–656 (2003).
18. Grand, R. J. *et al.* The high levels of p53 present in adenovirus early region 1-transformed human cells do not cause up-regulation of MDM2 expression. *Virology* **210**, 323–334 (1995).
19. Tachibana, M., Sugimoto, K., Fukushima, T. & Shinkai, Y. SET domain-containing protein, G9a, is a novel lysine-preferring mammalian histone methyltransferase with hyperactivity and specific selectivity to lysines 9 and 27 of histone H3. *J. Biol. Chem.* **276**, 25309–25317 (2001).
20. Otwinowski, Z. & Minor, W. in *Data Collection and Processing* (eds Sawyer, L., Isaacs, N. & Bailey, S.) 552–562 (SERC Daresbury Laboratory, Warrington, 1993).
21. CCP4. The CCP4 suite: programs for protein crystallography. *Acta Crystallogr. D* **50**, 760–763 (1994).
22. Jones, T. A., Zhou, J. Y., Cowan, S. W. & Kjeldgaard, M. Improved methods for building protein models in electron density maps and the location of errors in these models. *Acta Crystallogr. A* **47**, 110–119 (1991).

**Supplementary Information** accompanies the paper on [www.nature.com/nature](http://www.nature.com/nature).

**Acknowledgements** We thank L. Vales for comments on the manuscript. We also thank S. L. Berger and members of the Reinberg laboratory, especially A. Kuzmichev and K. Sarma for discussions. We also thank E. White for discussions and P. Chumakov for the gift of the lentivirus LSL–GFP vector, and A. Ivanov for generation of the siRNA-Set9 U2OS cell line. We thank S. Martin for assistance with binding experiments. The GRASP centre at Tufts is acknowledged for providing excellent technical support. This work was supported by a grant from the NIH and the Howard Hughes Medical Institute (D.R.). N.A.B. acknowledges support from the Charlton Award. S.J.G. acknowledges support from the Medical Research Council and from the Association for International Cancer Research.

**Competing interests statement** The authors declare that they have no competing financial interests.

**Correspondence** and requests for materials should be addressed to D.R. (reinbedf@UMDNJ.EDU) or N.A.B. (nbarlev@tufts-nemc.org). Coordinates have been deposited in the Protein Data Bank under accession code 1XQH.